SHAPE OPTIMAL DESIGN OF A RADIATING FIN[1,2]

M.C.Delfour
Centre de recherche de mathématiques appliquées
Université de Montréal
C.P. 6128, Succ.A
Montréal, Québec H3C 3J7

G. Payre
Département de Génie Chimique
Université de Sherbrooke
Sherbrooke, Québec
Canada J1K 2R1

J.-P. Zolésio
Département de Mathématiques
Université de Nice
06034 - Nice - Cédex
France

1. INTRODUCTION. Current trends indicate that future communications satellites and spacecrafts will grow ever larger, consume ever more electrical power, and dissipate larger amounts of thermal energy. Various techniques and devices can be employed to condition the thermal environment for payload boxes within a spacecraft, but it is desirable to employ those which offer good performance for low cost, low weight and high reliability.

A thermal radiator (or radiating fin) which accepts a given thermal power flux (TPF) from a payload box and radiates it directly to space, can offer good performance and high reliability at low cost. However without careful design, such a radiator can be unnecessarily bulky and heavy. It is the mass-optimized design of the thermal radiator which is the problem at hand. We may assume that the payload box presents a uniform TPF (typ. 0.1 to 1.0 W/cm^2) into the radiator at the box/radiator interface. The radiating surface is a second surface mirror which consists of a sheet of glass whose inner surface has silver coating. We may assume that the TPF out of the radiator/space interface is governed by the T^4 radiation law, although we must account also for a constant TPF (typ. 0.01 W/cm^2) into this interface from the sun. Any other surfaces of the radiator may be treated as adiabatic. Two constraints restrict freedom in the design of the thermal radiator:

(i) The maximum temperature at the box/radiator interface is not to exceed some constant (typ. 50°C), and

(ii) no part of the radiator is to be thinner than some constant (typ. 1mm).

A similar problem with a convective rather than a radiative condition has been considered by G.E.Schneider, M.M.Yovanovich and R.L.D.Cane [1] in connection with the cooling of banks of electronic circuitry where extensive use is made of integrated circuit devices. This work is also connected with the design of solar collectors and collector plates.

Shape optimal design techniques (cf. J.Céa [1,2,3]) have been successfully used in the design of mass-optimized thermal diffusers (cf. M.Delfour, F.Payre and J.P.Zolesio [1], and Ph.Destuynder [1]).

---

1. This problem has been suggested by A.S.Jones (Spar Aerospace Ltd., Toronto, Canada.)The above detailed statement has been provided by Dr.V.A.Wehrle (Communications Research Centre, Department of Communications, Ottawa, Canada).

2. This research has been supported by the Natural Sciences and Engineering Research Council of Canada, Strategic Grant G-0654 in Communications.

In this paper we present an efficient iterative method of solving the finite element approximation to the non-linear boundary value problem describing the temperature distribution in the radiating fin. This basic tool will be used many times to find the solution of the optimal design problem.

For the optimal design problem, the theory and gradient computations are obtained for the finite element model.
Shapes are restricted to a family of polygonal domains characterized by a finite number of shape parameters. Gradient computations involve partial derivatives of the position of the nodes with respect to the shape parameters and partial material derivatives of the state variable with respect to the position of each node. Both ingredients are combined to obtain the gradient of the penalized cost function with respect to the shape parameters. A few steps of some very preliminary computations are presented. However, at this stage, the program has not yet been carefully checked and is not completely operational.

Notation. Let $\mathbb{R}$ be the field of all real numbers. For an integer $K \geq 1$, $\mathbb{R}^K$ will be the K-dimensional Euclidean space. Given an open domain $\Omega \subset \mathbb{R}^K$, $L^p(\Omega)$ will be the space of p-integrable functions from Ω into $\mathbb{R}$, $1 \leq p \leq \infty$, and $L^\infty(\Omega)$ the space of essentially bounded functions from Ω into $\mathbb{R}$. $W^{1,p}(\Omega)$, $1 \leq p \leq \infty$, will denote the Sobolev space of $L^p(\Omega)$ functions with distributional derivatives of the first order in $L^p(\Omega)$. Define $H^1(\Omega) = W^{1,2}(\Omega)$. $C^0(\Omega)$ will denote the space of bounded continuous functions from Ω into $\mathbb{R}$.

2. STATEMENT OF THE PROBLEM.

We assume that the radiator is a volume Ω symmetrical about the z-axis (cf. Figure 1) whose boundary surface Σ is made up of three regular pieces: the contact surface Σ_1 (a disk perpendicular to the z-axis with center at the point $(r,z) = (0,0)$, the lateral adiabatic surface Σ_2 and the radiating surface Σ_3 (a disk perpendicular to the z-axis with center at $(r,z) = (0,L)$). More precisely

$$\Sigma_1 = \{(x,y,z)\,|\,z=0 \text{ and } x^2+y^2 \leq R_0^2\}, \quad \Sigma_2 = \{(x,y,z)\,|\,x^2+y^2=R(z)^2,\ 0 \leq z \leq L\}$$

$$\Sigma_3 = \{(x,y,z)\,|\,z=L,\ x^2+y^2 \leq R(L)^2\} \tag{1}$$

where the radius $R_0 > 0$ (typ. 10cm) the length $L > 0$ and the function

$$R:[0,L] \to \mathbb{R}, \quad R(0) = R_0, \quad R(z) > 0, \quad 0 \leq z \leq L \tag{2}$$

are given. ($\mathbb{R}$, the field of real numbers).

The temperature distribution (in Kelvin degrees) over this volume Ω is the solution of the stationary heat equation

$$\Delta T = 0 \quad \text{(the Laplacian of T)} \tag{3}$$

with the following boundary conditions on the surface $\Sigma = \Sigma_1 \cup \Sigma_2 \cup \Sigma_3$ (the boundary of Ω):

$$k\,\frac{\partial T}{\partial n} = q_{in} \text{ on } \Sigma_1, \quad k\,\frac{\partial T}{\partial n} = 0 \text{ on } \Sigma_2, \quad k\,\frac{\partial T}{\partial n} + \sigma\varepsilon T^4 = q_s \text{ on } \Sigma_3, \tag{4}$$

where n always denotes the outward normal to the boundary surface Σ and $\partial T/\partial n$ is the normal derivative on the boundary surface Σ. The parameters appearing in (1) to (6) are k = thermal conductivity (1.8 W/cm×°C), q_{in} = uniform inward thermal power flux at the contact surface (typ. 0.1 to 1.0 W/cm^2), σ = Boltzmann's constant (5.67×10^{-8} W/m^{2}K^4), ε = surface emissivity (typ. 0.8), q_s = solar inward thermal power flux (0.01 W/cm^2).

The optimal design problem consists in minimizing the volume

(5) $$J(R,L) = \pi\int_0^L R(z)^2 dz$$

over all lengths $L > 0$ and shape functions R subject to the constraint

(6) $$T(x,y,z) \le T_f \quad (\text{typ. } 50°\text{C}), \quad \forall\ (x,y,z) \in \Omega.$$

In the present analysis we drop the requirement (ii) in section 1.

3. SCALING AND VARIATIONAL FORMULATION OF THE NON-LINEAR BOUNDARY VALUE PROBLEM. It is convenient to introduce the following changes of variables (cf. Figure 2)

(7) $$\zeta = z/L, \quad \xi_1 = x/R_0, \quad \xi_2 = y/R_0, \quad \lambda = L/R_0$$

(8) $$y(\xi_1,\xi_2,\zeta) = \lambda^{1/3}(\sigma\varepsilon R_0/k)^{1/3}\, T(R_0\xi_1, R_0\xi_2, L\zeta).$$

This defines the *new shape function*

(9) $$\rho(\zeta) = R(L\zeta)/R_0, \quad \rho:[0,1] \to R_+, \quad \rho(0) = 1, \quad \rho(\zeta) > 0 \text{ in } [0,1],$$

and the *dimensionless parameter* $\lambda > 0$. The new volume $\tilde{\Omega}$ and its boundary $\tilde{\Sigma}$ are given by

(10) $$\tilde{\Omega} = \{(\xi_1,\xi_2,\zeta)\,|\,0 < \zeta < 1,\ \xi_1^2+\xi_2^2 < \rho(\zeta)^2\}, \quad \tilde{\Sigma} = \tilde{\Sigma}_1 \cup \tilde{\Sigma}_2 \cup \tilde{\Sigma}_3$$

(11) $$\tilde{\Sigma}_1 = \{(\xi_1,\xi_2,0)\,|\,\xi_1^2+\xi_2^2 \le 1\}, \quad \tilde{\Sigma}_2 = \{(\xi_1,\xi_2,\zeta)\,|\,0\le\zeta\le1,\ \xi_1^2+\xi_2^2=\rho(\zeta)^2\}$$
$$\tilde{\Sigma}_3 = \{(\xi_1,\xi_2,1)\,|\,\xi_1^2+\xi_2^2 \le \rho(1)^2\}.$$

Equations (3) and (4) become

(12) $$A(y) = -[\lambda^2(\frac{\partial^2 y}{\partial\xi_1^2} + \frac{\partial^2 y}{\partial\xi_2^2}) + \frac{\partial^2 y}{\partial\zeta^2}] = 0 \text{ in } \tilde{\Omega},$$

(13) $$\frac{\partial y}{\partial\nu_A} = q_{in} \text{ on } \tilde{\Sigma}_1, \quad \frac{\partial y}{\partial\nu_A} = 0 \text{ on } \tilde{\Sigma}_2, \quad \frac{\partial y}{\partial\nu_A} + y^4 = \tilde{q}_s \text{ on } \tilde{\Sigma}_3$$

where

(14) $$\beta = (\sigma\varepsilon R_0^4/k^4)^{1/3}, \quad \tilde{q}_{in} = \beta q_{in}\lambda^{4/3}, \quad \tilde{q}_s = \beta q_s\lambda^{4/3}.$$

The solution y only depends on λ, βq_{in}, βq_s and the shape function ρ. Once βq_{in} and βq_s have been fixed, the *optimal design problem* consists in finding the parameter λ and the shape function ρ which minimizes the volume

(15) $$J(\lambda,\rho) = \pi\lambda\int_0^1 \rho(\zeta)^2 d\zeta$$

subject to the constraint

(16) $$\sup\{y(\sigma)\,|\,\sigma \in \tilde{\Sigma}_1\} \le \tilde{y}_1, \quad \tilde{y}_1 = T_f(\sigma\varepsilon R_0/k)^{1/3}\lambda^{1/3}.$$

It was shown in Delfour, Payre and Zolesio [2], that the solution

$$y(r,\zeta) = y(\xi_1,\xi_2,\zeta), \quad r = \sqrt{\xi_1^2+\xi_2^2} \tag{17}$$

(in cylindrical coordinates) of the above boundary-value problem coincides with the minimizing element of the functional j

$$j(\varphi) = \frac{1}{2}a_\lambda(\varphi,\varphi)+\int_0^{\rho(1)} 2\pi r dr[\frac{1}{5}|\varphi|^5-\tilde{q}_s\varphi]-\int_0^1 2\pi r dr \tilde{q}_{in}\varphi \tag{18}$$

$$a_\lambda(\varphi,\psi) = \int_0^1\int_0^{\rho(\zeta)}[\lambda^2 \frac{\partial\varphi}{\partial r}\frac{\partial\psi}{\partial r} + \frac{\partial\varphi}{\partial\zeta}\frac{\partial\psi}{\partial\zeta}]2\pi r dr d\zeta, \tag{19}$$

over the function space

$$W(A) = \{\varphi|\sqrt{r}\,\varphi,\ \sqrt{r}\,\frac{\partial\varphi}{\partial r},\ \sqrt{r}\,\frac{\partial\varphi}{\partial\zeta} \in L^2(A),\ \sqrt[5]{r}\,\varphi|_{S_3} \in L^5(S_3)\}. \tag{20}$$

The functional j is Gateau differentiable and its derivative at φ in the ψ direction is given by

$$dj(\varphi;\psi) = a_\lambda(\varphi,\psi)+\int_0^{\rho(1)} 2\pi r dr[|\varphi|^3\varphi-\tilde{q}_s]\psi-\int_C^1 2\pi r dr\tilde{q}_{in}\psi. \tag{21}$$

The minimizing element y is completely characterized by the variational equation

$$dj(y;\psi) = 0, \quad \forall\psi \in W(A). \tag{22}$$

Moreover the function y is positive over the closure $\bar{A}$ of A. The Hessian can also be explicitly computed:

$$d^2j(\varphi;\psi,\eta) = a_\lambda(\eta,\psi)+\int_0^{\rho(1)} 2\pi r dr\ 4|\varphi|^2\varphi\eta\psi. \tag{23}$$

4. FINITE ELEMENT APPROXIMATION OF THE NLBVP. The function space W(A) is approximated in two steps. First an approximation ρ_h of the shape function ρ as a continuous piecewise linear function. The function ρ_h generates an approximation A_h

$$A_h = \{(r,\zeta)|0 < \zeta < 1, \quad 0 < r < \rho_h(\zeta)\} \tag{24}$$

to the cross-section A; by revolution about the ζ-axis, A_h generates the volume $\tilde{\Omega}_h$.

Then, define a triangulation τ_h on the cross-section A_h and associate with it the finite element approximation

$$W_h = \{\varphi_h|\varphi_h \in C^0(\bar{A}_h),\ \varphi_h \text{ linear on each triangle in } \tau_h\}. \tag{25}$$

The finite element approximation y_h of the minimizing function y is given by the solution of the variational equation

$$dj_h(y_h;\psi_h) = 0, \quad \forall\psi_h \in W_h, \tag{26}$$

where j_h is defined by (18) with ρ_h and A_h instead of ρ and A. Various non-linear programming algorithms have been developed in Delfour-Payre-Zolesio [2] to compute y_h. In this paper we use the following new iterative scheme. Given the real function

$$f(x) = (|x|^3x-c^4)/(x-c), \quad c^4 = \tilde{q}_s, \tag{27}$$

we consider the following sequence of minimization problems: at step $n \geq 1$, y_n is known and $y_{n+1} \in W_h$ is constructed as follows:

$$j_n(y_{n+1}) = \mathrm{Inf}\{j_n(\varphi_h)|\varphi_h \in W_h\}, \tag{28}$$

where

$$(29)\qquad j_n(\varphi) = \frac{1}{2}a_\lambda(\varphi,\varphi) + \int_0^{\rho_h(1)} f(y_n)\frac{1}{2}|\varphi-c|^2 2\pi r dr - \int_0^1 \tilde{q}_{in}\varphi 2\pi r dr.$$

5. DISCRETE OPTIMAL DESIGN PROBLEM. Given the function ρ_h, the cross-section A_h and the triangulation τ_h, the temperature distribution y_h in W_h is the solution of (26). The "discrete optimal design problem" is the same as the one in section 3 except for the fact that ρ is replaced by ρ_h in (15) and (16). This constrained problem is solved by penalization of (16):

$$(30)\qquad J_\varepsilon(\lambda,\tau_h) = J(\lambda,\rho_h) + \frac{1}{\varepsilon}\int_0^1\{[y_h-\tilde{y}_1]^+\}^2 2\pi r dr, \quad \varepsilon > 0$$

where $[u]^+ = \max\{u,0\}$ and τ_h indicates that J_ε depends not only on ρ_h but also on the triangulation through the state y_h.

6. CONSTRUCTION OF THE TRIANGULATION τ AND INTRODUCTION OF THE SHAPE PARAMETERS. For simplicity we drop the subscript "h" associated with the "discrete problem". It has been noticed that the state y does not only depend on the surface A but also on the chosen triangulation τ and, a fortiori, on the set of nodes $\vec{M}=\{M_i | 1\le i\le m\}$ (m, an integer) which defines τ. It is not computationally and physically desirable to leave all the nodes completely free. So we introduce a fixed set of shape parameters, $\vec{\ell} = \{\ell_k | 1\le k\le p+q\}$ (p and q, integers) to "control" $\vec{M}$.

The domain A is divided into two parts by introducing a focus $F = (F_r,0)$, $F_r > 1$, and two sets of nodes $\vec{E}_p = \{E_i | 0 \le i \le p\}$ $(E_0 = (0,0),\ E_p = (F_r,1))$ and $\vec{E}_q = \{E_i | p < i \le p+q\}$ $(E_i = (E_{ir},1))$ distributed along the ζ-axis and the boundary S_3 (cf. Figure 3). In the first part, rays are drawn from F to each node E_i, $0 \le i \le p$; in the second part, lines are drawn parallel to the ζ-axis through each point of $\vec{E}_q$. The boundary S_2 and, a fortiori, the function ρ are defined by the set of positive parameters $\vec{\ell}$ in the following way. The boundary points are

$$(31)\qquad B_i = \begin{cases} E_i + (F-E_i)\ell_i/|F-E_i|, & 1 \le i \le p, \\ E_i - (0,\ell_i), & p < i \le p+q \,. \end{cases}$$

By joining the points $B_0 = (1,0)$, B_1, $B_2,\ldots$, B_{p+q} and E_{p+q} by straight lines, the function ρ_h and the boundary S_2 are generated. In the actual computations the first component of the node E_{p+q} was also considered as a shape parameter controlling the nodes E_i, $p < i < p+q$. However, for lack of space, we do not describe this construction here.

7. ELEMENTS IN THE COMPUTATION OF THE GRADIENT OF THE COST FUNCTION WITH RESPECT TO THE SHAPE PARAMETERS. Though the surface A is completely determined by the boundary nodes, the finite element state y depends on the whole triangulation τ and thence on the set of nodes $\vec{M}$. In general we can write

$$(32)\qquad y = y(\vec{M}),\quad A = A(\vec{M}) \text{ and } J_\varepsilon = J_\varepsilon(A(\vec{M})).$$

By construction the nodes $\vec{M}$ are completely determined by the fixed nodes $\vec{E}_p$, $\vec{E}_q$ and

F and the shape parameters $\vec{\ell}$. Therefore we write

(33) $$\vec{M} = \vec{M}(\vec{\ell}),$$

and the cost function becomes a function L of $\vec{\ell}$

(34) $$L(\vec{\ell}) = J_\varepsilon(A(\vec{M}(\vec{\ell}))).$$

As a result, using the chain rule,

(35) $$\frac{\partial L}{\partial \ell_k} = \sum_{i=1}^{m} \left[\frac{\partial J_\varepsilon}{\partial r_i}\frac{\partial r_i}{\partial \ell_k} + \frac{\partial J_\varepsilon}{\partial \zeta_i}\frac{\partial \zeta_i}{\partial \ell_k}\right], \quad M_i = (r_i,\zeta_i), \quad 1 \le r \le m,$$

where the pairs $\{(\partial J_\varepsilon/\partial r_i,\ \partial J_\varepsilon/\partial \zeta_i)\,|\,1 \le i \le m\}$ are the partial material derivatives of J_ε with respect to the node M_i and the partial derivatives of r_i and ζ_i with respect to ℓ_k. The computation of (35) involves the *partial material derivatives* $(\dot{y}_{r_i},\dot{y}_{\zeta_i})$ of the state y with respect to the position of each node M_i and the introduction of an adjoint state. This will require the construction of appropriate deformation fields.

8. <u>PARTIAL MATERIAL DERIVATIVES</u>. We briefly recall the speed method for boundary value problems over smooth domains Ω. Given a smooth deformation vector field V defined in a neighbourhood of Ω, each point X in Ω at time t=0 is transported into a point x(t) at time t > 0 through the differential equation

(36) $$dx(t)/dt = V(t,x(t)), \quad x(0) = X.$$

This induces a smooth transformation $T_t(V)X = x(t)$ which maps Ω onto $\Omega_t = T_t(V)\Omega$. The Eulerian derivative of the cost function J at Ω for the field V is defined as (cf. J.P.Zolésio [1,2])

(37) $$dJ(\Omega;V) = (d/dt)J(\Omega_t)|_{t=0}.$$

In the discrete case, the state y depends on the nodes $\vec{M}$ through the triangulation τ. Given a node $M_i = (r_i,\zeta_i)$ and a small $t > 0$ we perturb the nodes $\vec{M}$ into

(38) $$\vec{M}^t_{r_i} = \{M_j+t(\delta_{ij},0)\,|\,1 \le j \le m\} \quad\text{or}\quad \vec{M}^t_{\zeta_i} = \{M_j+t(0,\delta_{ij})\,|\,1 \le j \le m\}$$

where δ_{ij} is the Kronecker index function. Now we want to construct in each case vector fields which will transport triangles in τ onto a new set of triangles τ^t and the shape functions $\vec{e} = \{e_j\,|\,1 \le j \le m\}$ in W_h for τ onto shape functions $\vec{e}^t = \{e^t_j\,|\,1 \le j \le m\}$ in W^t_h for τ^t:

(39) $$e_j(M_i) \quad (\text{resp. } e^t_j(M^t_i)) = \delta_{ij}, \quad 1 \le i,j \le m.$$

J.P.Zolésio [4] has shown that an appropriate choice is

(40) $$V_{r_i}(r,\zeta) = (e_i(r,\zeta),0) \quad (\text{resp. } V_{\zeta_i}(r,\zeta) = (0,e_i(r,\zeta))).$$

Such a field maps each triangle of τ onto a triangle of τ^t and each basis element e_j onto a basis element e^t_j. Moreover if y_t is a solution of the boundary value problem in W^t_h, then

(41) $$y^t_{r_i} = y_t \circ T_t(V_{r_i}) \quad (\text{resp. } y^t_{\zeta_i} = y_t \circ T_t(V_{\zeta_i}))$$

belongs to W_h. Thus the *partial material derivative* of y is an element of W_h

(42) $$\dot{y}_{r_i} = dy^t_{r_i}/dt|_{t=0} \quad (\text{resp. } \dot{y}_{\zeta_i} = dy^t_{\zeta_i}/dt|_{t=0})$$

and the *partial Eulerian derivative* of J_ε is given by

(43) $$\partial J_\varepsilon/\partial r_i = dJ_\varepsilon(A;V_{r_i}) \quad (\text{resp. } \partial J_\varepsilon/\partial\zeta_i = dJ_\varepsilon(A;V_{\zeta_i})).$$

It can be shown that for vector fields $V = (V^r, V^\zeta)$ of this type (that is, V_{r_i} or V_{ζ_i}), the Eulerian derivative of J_ε is given by (cf. J.P.Zolésio [1,4])

(44) $$dJ_\varepsilon(A;V) = \int_A 2\pi\,[V^r + r(\partial_r V^r + \partial_\zeta V^\zeta)]\,dr\,d\zeta + \int_A \langle \mathcal{A}'\nabla y, \nabla p\rangle 2\pi\,dr\,d\zeta + \int_{S_3}(y^4 - \tilde{q}_s)\,p\,(V^r + r\partial_r V^r)\,dr,$$

where ∂_r and ∂_ζ denote partial derivatives and $\mathcal{A}'$ is the 2×2 matrix

(45) $$\mathcal{A}' = (\mathrm{div}V)B - (DV)B - B(DV)^* + V^r E, \quad B = rE, \quad E = \begin{bmatrix} \lambda^2 & 0 \\ 0 & 1 \end{bmatrix}$$

DV is the Jacobian matrix of V, $(DV)^*$ its transpose and p is the solution in W_h of the variational equation

(46) $$d^2 j(y;p,\psi) + \frac{2}{\varepsilon}\int_0^1 [y - \tilde{y}_1]^+ \psi\, 2\pi r\,dr = 0, \quad \forall\psi \in W_h.$$

The substitution of $V = V_{r_i}$ (resp. $V = V_{\zeta_i}$) will yield an explicit expression for (43) in terms of e_i, y and $\overset{1}{p}$. Combining this with the chain rule (35), the optimal design problem can be solved by any gradient method.

9. NUMERICAL RESULTS. The results presented here are very preliminary. They only show a few iterations with a computer program which has not yet been carefully checked and which is not completely operational. The triangulation is made up of 167 nodes and 275 elements (linear on each triangle).

The tests have been divided into two steps. Firstly the geometry of the boundary S_2 has been chosen as two straight lines (cf. Figure 4): one from (1,0) to (R,Z), $0 < Z < 1$ (R is the r-component of the point $E_{p+q} = (R,1)$) and one from (R,Z) to $E_{p+q} = (R,1)$. After a series of evaluations of the volume and the constraint, the parameters λ, R and Z were chosen in the following way: $\lambda R_0 = L = 1$cm, ZL = 0,9 cm, $RR_0 = 18{,}75$ cm, $R_0 = 5$ cm. During the iterations, λ, R and Z were fixed and the algorithm began to dig into the surface S_2. Five such iterations are shown in Figure 5. The evolution of the volume, the constraint and the cost as a function of the iteration number are shown in Figure 6. The temperature profiles at iteration 5 are shown in Figure 7. The hottest profile is 49,75° on the side of the boundary $\tilde{\Sigma}_3$ near the ζ-axis. The shape obtained at iteration 5 is not necessarily optimal since iterations were not continued. Nevertheless the algorithm seems to converge towards a "physical" solution.

REFERENCES

J. Céa [1], Une méthode numérique pour la recherche d'un domaine optimal, Publication IMAN, Université de Nice, 1976.

[2], Optimization, theory and algorithm, Tata Institute, Springer Verlag, 1978.

[3], Problem of Shape Optimal Design, pp. 1005-1048; Numerical Methods of Shape Optimal Design, pp. 1049-1088, in "Optimization of distributed parameter structures", Vol.II, E.Haug, and J.Céa, eds., Sijthoff and Noordhoff, Alphen aan den Rijn, The Netherlands, 1981.

M.C. Delfour, G.Payre and J.P. Zolésio [1], Optimal design of a minimum weight thermal diffuser with constraint on the output thermal power flux, J.Applied Math. and Optimization 9 (1983), 225-262.
[2], Optimal design of a radiating fin for communications satellites, Proc. IFAC Workshop on Appl.Nonlinear Programming to Optimization and Control, H.Rauch,ed., San Francisco, U.S.A., June 1983 (to appear).
Ph.Destuynder [1], Etude théorique et numérique d'un algorithme d'optimisation de structures. Thèse de docteur ingénieur, Université de Paris VI, 1976.
G.E.Schneider, M.M. Yovanovich and R.L.D. Cane [1], Thermal resistance of a convectively cooled plate with nonuniform applied flux, J.Spacecraft and Rockets 17, 372-376, 1980.
J.P.Zolésio [1], The material derivative (or speed) method for shape optimization. In "Optimization of distributed parameter structures" Vol.II, pp. 1089-1151, E.J.Haug and J.Céa,eds., Sijthoff and Noordhoff, Alphen aan den Rijn, The Netherlands, 1981.
[2], Identification de domaines par déformation. Thèse de doctorat d'état, Université de Nice, 1979.
[3] In Proceedings of a conference held at Murat le Quaire, A.Auslender,ed., pp. 200-230, Lecture Notes in Economical and Mathematical Systems no.14, Springer Verlag, New York, 1977.
[4], Les dérivées par rapport aux noeuds des triangularisations et leur utilisations en identification de domaine, Ann.Sc.Mat.Québec, to appear.

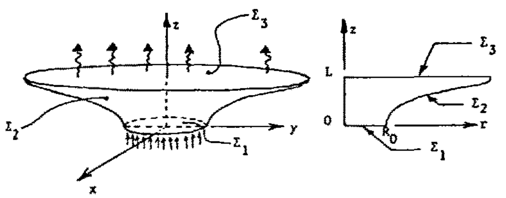

Figure 1. Domain Ω and its generating surface.

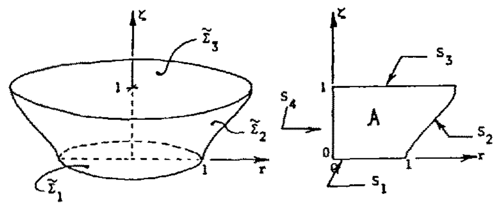

Figure 2. Domain $\tilde{\Omega}$ and its generating surface A.

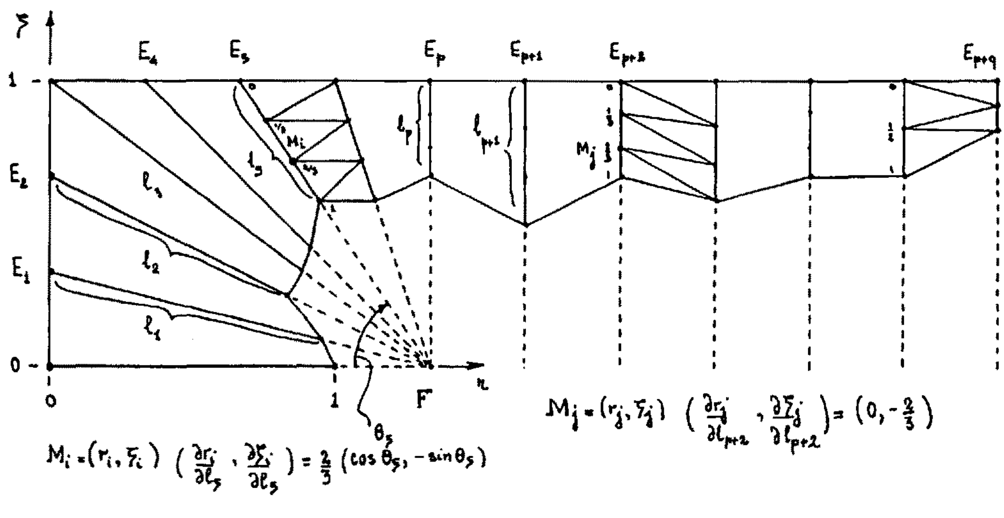

Figure 3. Triangulation τ and shape parameter $\tilde{\ell}$.

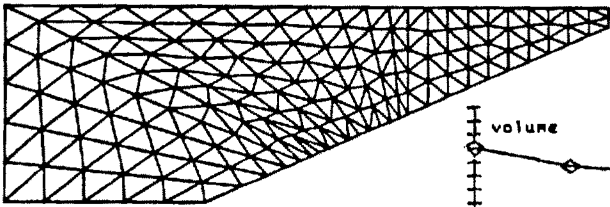

Figure 4. Triangulation.

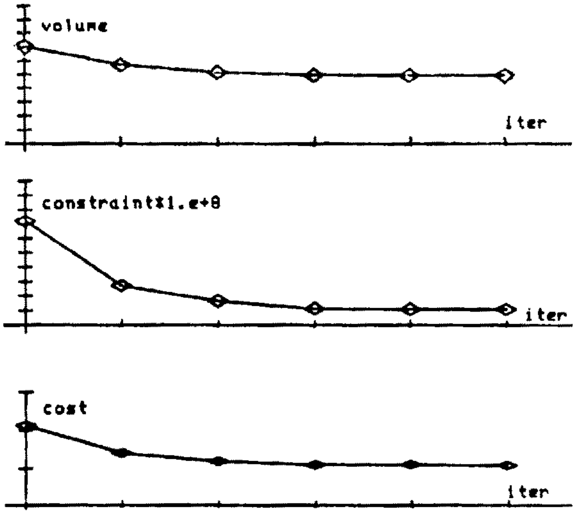

Figure 6. Volume, constraint and penalized cost versus iteration number.

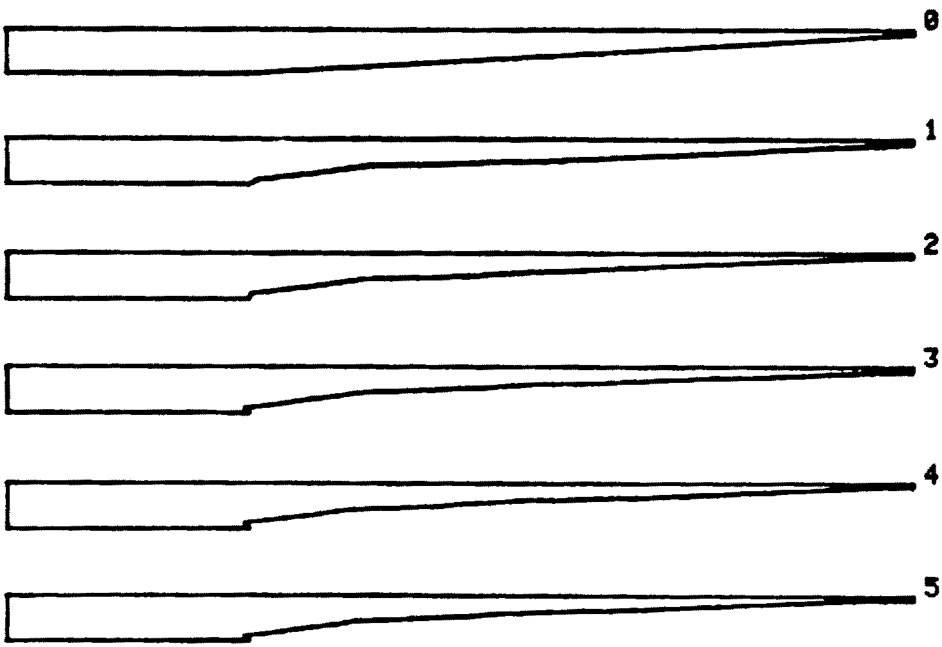

Figure 5. Successive shapes for the second set of five iterations.

Figure 7. Temperature profiles at iteration 5.